Achieving broadband near-infrared emission with superior anti-thermal quenching by optimizing excited-state population of $Cr^{3+}$ in $Gd_3ScGa_4O_{12}$ garnet phosphors

Wangyu Liu[a], Lifang Yuan[b], Haoyi Wu[a], Huafeng Dong[a], Yahong Jin*[ac]

[a]School of Physics and Optoelectronic Engineering, Guangdong University of Technology, WaiHuan Xi Road, No. 100, Guangzhou 510006, China.
[b]School of Electronics and Communications, Guangdong Mechanical & Electrical Polytechnic, Guangzhou 510515, China
[c]Guangdong Provincial Key Laboratory of Sensing Physics and System Integration Applications, WaiHuan Xi Road, No. 100, Guangzhou 510006, China.
E-mail: yhjin@gdut.edu.cn

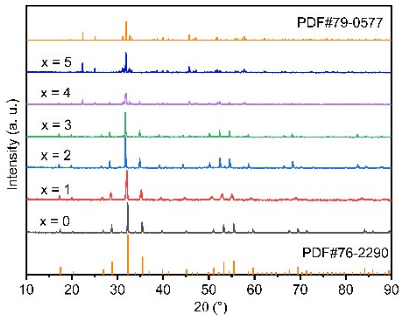


**Fig. S1.** XRD patterns of $Gd_3Sc_xGa_{5-x}O_{12}$:0.08$Cr^{3+}$ (x = 0–5).

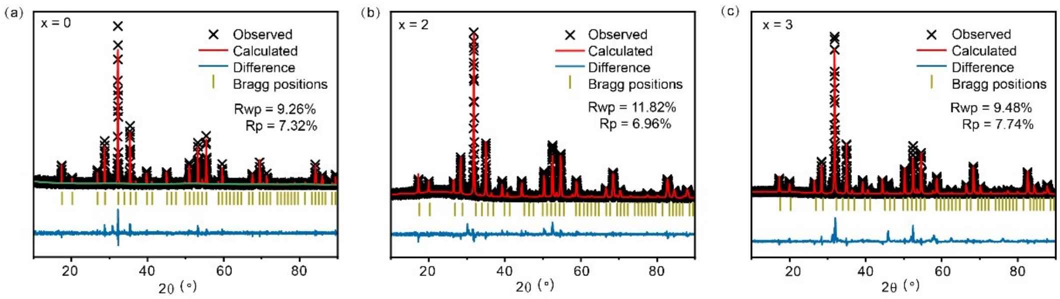


**Fig. S2.** (a–c) XRD Rietveld refinement of $Gd_3Sc_xGa_{5-x}O_{12}$ (x = 0, 2, 3).

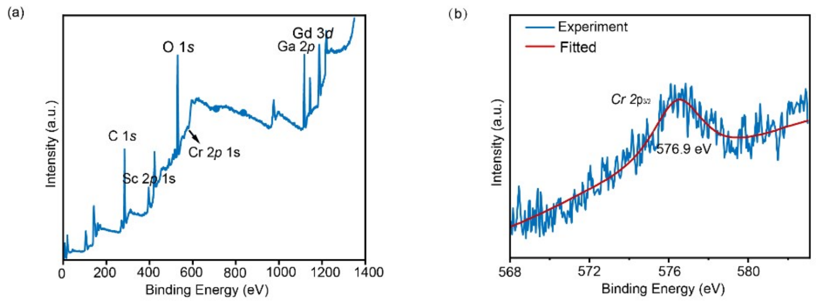


**Fig. S3.** (a) XPS full spectrum and (b) Cr 2p scan of $Gd_3ScGa_4O_{12}$:$0.08Cr^{3+}$.

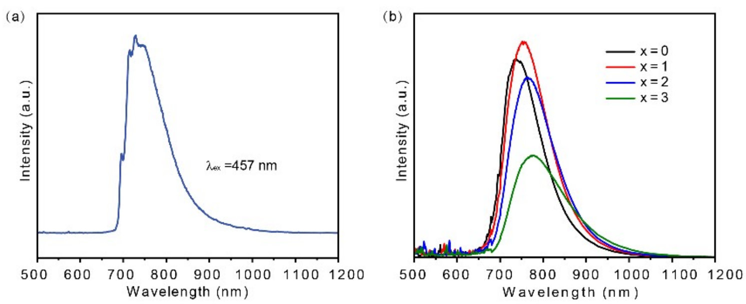


**Fig. S4.** (a) Emission spectrum of $Gd_3ScGa_4O_{12}$:0.08$Cr^{3+}$ at 77 K. (b) Relative emission intensity of $Gd_3Sc_xGa_{5-x}O_{12}$:0.08$Cr^{3+}$ (x = 0–3).

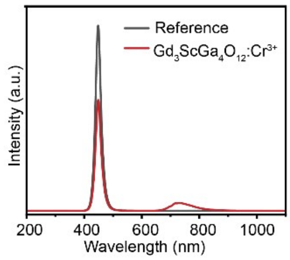


**Fig. S5**. IQE (82.75%), EQE (28.19%), and absorption coefficient (34.07%) of $Gd_3ScGa_4O_{12}$:0.08$Cr^{3+}$.

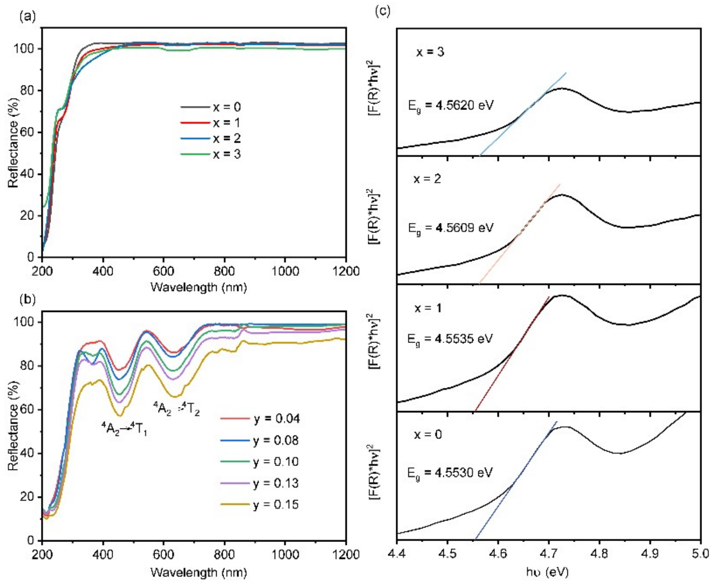


**Fig. S6.** (a) DRS of $Gd_3Sc_xGa_{5-x}O_{12}$ (x = 0–3). (b) DRS of $Gd_3ScGa_4O_{12}$:$yCr^{3+}$ (y = 0.04–0.15). (c) The estimated optical band gaps of $Gd_3Sc_xGa_{5-x}O_{12}$ (x = 0–3).

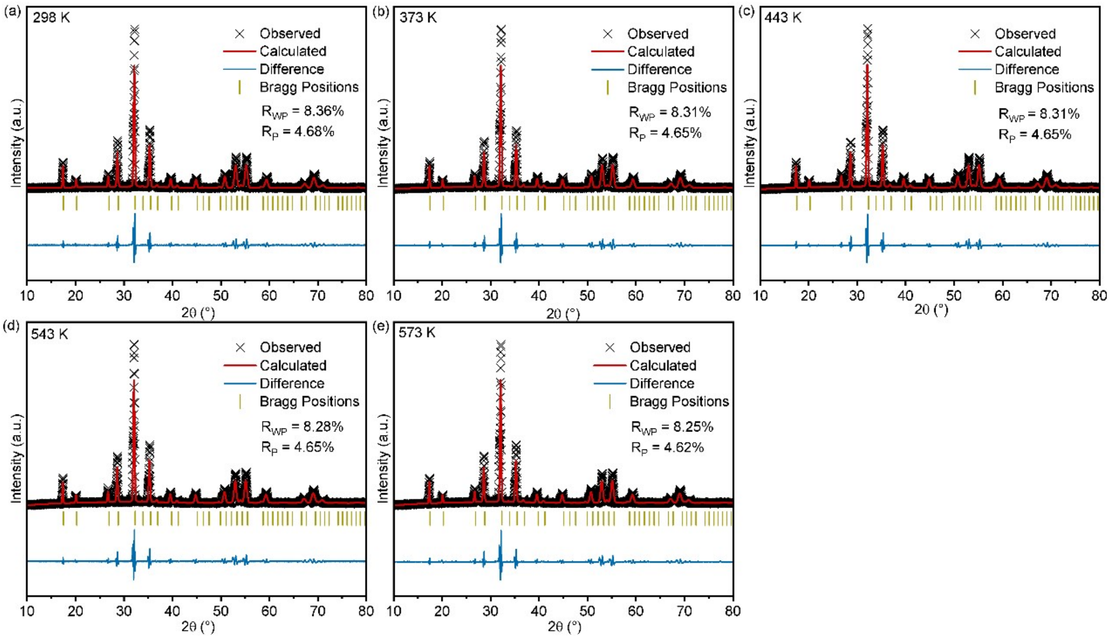


**Fig. S7.** XRD Rietveld refinement of (a) $Gd_3ScGa_4O_{12}$:0.08$Cr^{3+}$ at (a) 25 °C, (b) 100 °C, (c) 170 °C, (d) 270 °C, (e) 300 °C.

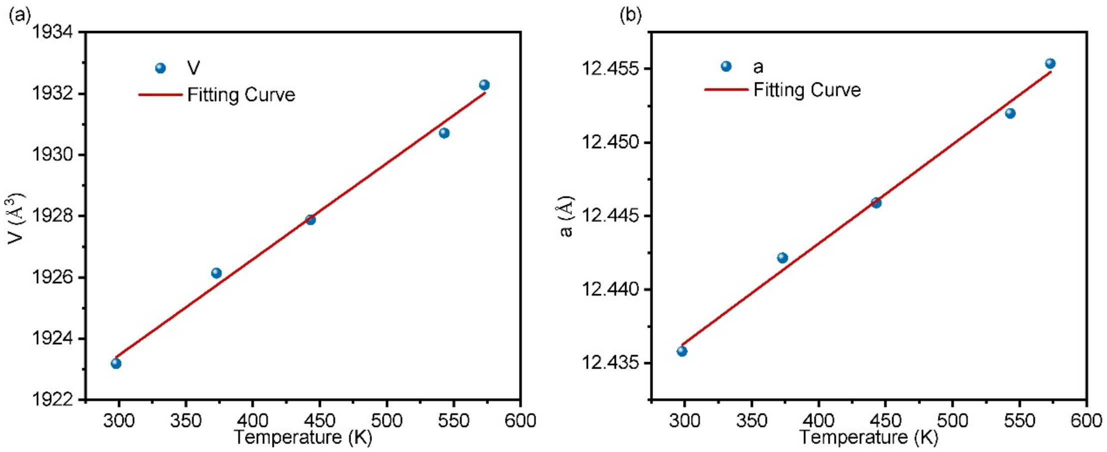


**Fig. S8.** Temperature-dependent (a) volume and (b) lattice parameters for $Gd_3ScGa_4O_{12}$:0.08$Cr^{3+}$.

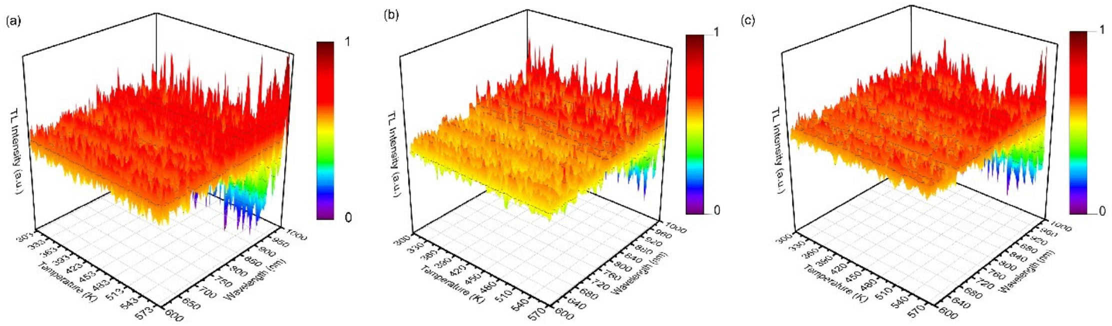

**Fig. S9.** Thermoluminescence curves of $Gd_3ScGa_4O_{12}$:0.08$Cr^{3+}$ measured without preheating (a) and with preheating at (b) 100 ℃ and (c) 150 ℃ under 460 nm excitation.

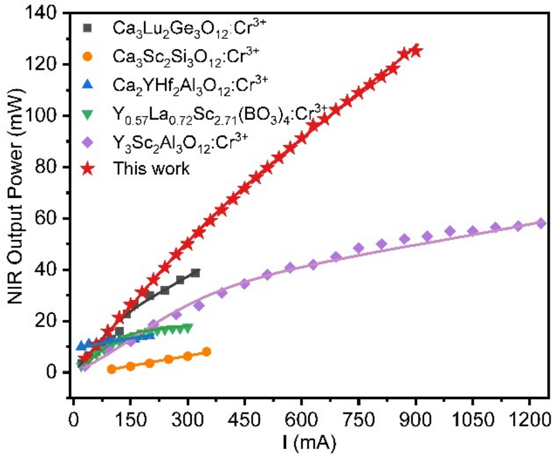


**Fig. S10.** A comparison of the NIR output power with other garnet NIR phosphors reported previously.[1-5]

**Table S1.** Crystallographic data of $Gd_3Sc_xGa_{5-x}O_{12}$ (x = 0–3).

| Samples | x = 0 | x = 1 | x = 2 | x = 3 |
|---|---|---|---|---|
| Crystal system | | Cubic | | |
| Space group | | $Ia\bar{3}d$ | | |
| a=b=c (Å) | 12.3691 | 12.4523 | 12.5496 | 12.5747 |
| α=β=γ | 90 | 90 | 90 | 90 |
| Volume (Å$^3$) | 1892.389 | 1930.835 | 1976.485 | 1988.344 |
| Sc-$O_6$ (Å) | 1.999 | 2.012 | 2.076 | 2.087 |
| $R_p$ | 0.0732 | 0.0731 | 0.0696 | 0.0774 |
| $R_{wp}$ | 0.0926 | 0.0936 | 0.1182 | 0.0948 |
| $\chi^2$ | 1.35 | 1.299 | 1.827 | 4.937 |
| Gd1 | (0.125,0.000,0.250) | (0.125,0.000,0.250) | (0.125,0.000,0.250) | (0.125,0.000,0.250) |
| Ga1 | (0.000,0.000,0.000) | (0.000,0.000,0.000) | (0.000,0.000,0.000) | (0.000,0.000,0.000) |
| Ga2 | (0.375,0.000,0.250) | (0.375,0.000,0.250) | (0.375,0.000,0.250) | (0.375,0.000,0.250) |
| O1 | (0.967,0.053,0.149) | (0.968,0.052,0.150) | (0.968,0.053,0.150) | (0.969,0.053,0.151) |
| Sc1 | (0.000,0.000,0.000) | (0.000,0.000,0.000) | (0.000,0.000,0.000) | (0.000,0.000,0.000) |

**Table S2.** The survey of ion-doped (excluding $Cr^{3+}$-doped) inorganic phosphors with anti-TQ performance.

| Host materials | Activators | Ex/Em (nm) | FWHM (nm) | IQE | $I_T/I_{RT}$ | Ref. |
|---|---|---|---|---|---|---|
| $Ba_2ZnGe_2O_7$ | $Bi^{3+}$ | 346/500 | 129 | – | 138%@423K | [6] |
| $Na_3Ca_4TeP_3O_{15}$ | $Tb^{3+}$, $Eu^{3+}$ | 376/545, 617 | | – | 109%@423K | [7] |
| $Lu_2SrAl_4SiO_{12}$ | $Eu^{2+}$ | 342/420 | | – | 106%@423K | [8] |
| $Sc_{1.8}Zr_{0.1}Nb_{0.1}W_{2.85}O_{11.7}$ | $Yb/Er^{3+}$ | 522/980 | | – | 114%@448K | [9] |
| $Ca_{3.6}In_{3.6}(PO_4)_6$ | $Dy^{3+}$ | 349/575 | | 30.3% | 108.2%@423K | [10] |
| $Ba_3EuAl_2O_{7.5}$ | $Eu^{3+}$ | 270/593 | | | 140%@443K | [11] |
| $Ca_2InSbO_6$ | $Eu^{3+}$ | 395/616 | | 82% | 114.5%@380K | [12] |
| $LaSc_3(BO_3)_4$ | $Eu^{3+}$ | 395/618 | | 88.3% | 129.2%@548K | [13] |
| $KAl_{11}O_{17}$ | $Mn^{2+}$ | 450/510 | ~50 | – | 160%@548K | [14] |
| $Cs_2MP_2O_7$ (M=Ba,Sr,Ca) | $Eu^{2+}$ | 360/548 | | 98.9% | 120%@448K | [15] |
| $Mg_3Y_2Ge_3O_{12}$ | $Eu^{3+}$, $Mn^{4+}$ | 420/660 | | – | 127%@500K | [16] |
| $CsMoO_2F_3$ | $Mn^{4+}$ | 450/633 | | 54% | 129.3%@423K | [17] |
| $LaAlO_3$ | $Ca^{2+}$, $Bi^{3+}$, $Mn^{4+}$ | 340/734 | | 89.3% | 103%@423K | [18] |
| $In_{0.5}Sc_{1.5}(MoO_4)_3$ | $Eu^{3+}$ | 246/615 | | 57.8% | 108.2%@473K | [19] |

**Table S3.** Crystallographic data of $Gd_3ScGa_4O_{12}$:0.08$Cr^{3+}$ at different temperatures.

| Materials | $Gd_3ScGa_4O_{12}$:0.08$Cr^{3+}$ | | | | |
|---|---|---|---|---|---|
| Measuring temperature/°C | 25 | 100 | 170 | 270 | 300 |
| Crystal system | | | Cubic | | |
| Space group | | | $Ia\bar{3}d$ | | |
| a=b=c (Å) | 12.4440 | 12.4498 | 12.4563 | 12.4652 | 12.4687 |
| α=β=γ | 90° | 90° | 90° | 90° | 90° |
| Volume (Å$^3$) | 1926.995 | 1929.669 | 1932.691 | 1936.864 | 1938.468 |
| Average bond length of Cr-O (Å) | 2.053 | 2.055 | 2.057 | 2.058 | 2.061 |
| Volume of $CrO_6$ octahedron (Å$^3$) | 11.4548 | 11.4942 | 11.5276 | 11.5486 | 11.6141 |
| $R_p$ | 0.0469 | 0.0466 | 0.0466 | 0.0466 | 0.0464 |
| $R_{wp}$ | 0.0838 | 0.0832 | 0.0833 | 0.0829 | 0.0827 |
| $\chi^2$ | 2.08 | 2.86 | 2.92 | 2.79 | 2.67 |

References:

[1] J. Feng, X. Wu, D. Zhu, J. Chen, Z. Mu, *Journal of Luminescence* **2022**, 252, 119379.

[2] Y. Zhou, X. Li, T. Seto, Y. Wang, *ACS Sustainable Chemistry & Engineering* **2021**, 9, 3145-3156.

[3] D. Huang, Q. Ouyang, H. Xiao, B. Wang, H. Lian, Q. Zeng, J. Lin, *Dalton Transactions* **2021**, 51, 908-916.

[4] D. Qian, Y. Jin, Y. Li, H. Wu, Y. Hu, *Applied Physics A* **2024**, 130, 233.

[5] H. Wu, L. Jiang, K. Li, C. Li, H. Zhang, *Journal of Materials Chemistry C* **2021**, 9, 11761-11771.

[6] Y. Wei, H. Yang, Z. Gao, X. Yun, G. Xing, C. Zhou, G. Li, *Laser & Photonics Reviews* **2021**, 15, 2000048.

[7] R. Song, R. Wang, X. Yang, X. Bian, H. Fu, *Applied Materials Today* **2024**, 38, 102246.

[8] T. Ying-Ying, Y. Zi-Han, W. Chun-Hao, W. Ting-Wei, L. Fa-Chun, *Journal of the American Ceramic Society* **2022**, 105, 5240.

[9] B. Fu, H. Yan, R. Li, L. Feng, Y. Yu, G. Gong, H. Huang, J. Liao, *Laser & Photonics Reviews* 2400739, doi.org/10.1002/lpor.202400739.

[10] R.-R. Wang, J. Zhang, Y.-J. Liu, G.-H. Li, G.-M. Cai, *Dalton Transactions* **2023**, 52, 5552.

[11] X. Bian, R. Wang, S. Li, Q. Shi, H. Fu, *Journal of Luminescence* **2023**, 257, 119768.

[12] X. Geng, Y. Xie, Y. Ma, Y. Liu, J. Luo, J. Wang, R. Yu, B. Deng, W. Zhou, *Journal of Alloys and Compounds* **2020**, 847, 156249.

[13] S. Wang, Y. Xu, T. Chen, W. Jiang, J. Liu, X. Zhang, W. Jiang, L. Wang, *Chemical Engineering Journal* **2021**, 404, 125912.

[14] Z. Zhou, H. Zhu, X. Huang, Y. She, Y. Zhong, J. Wang, M. Liu, W. Li, M. Xia, *Chemical Engineering Journal* **2022**, 433, 134079.

[15] Y. Wei, Z. Gao, S. Liu, S. Chen, G. Xing, W. Wang, P. Dang, A. A. Al Kheraif, G. Li, J. Lin, *Advanced Optical Materials* **2020**, 8, 1901859.

[16] Y. Wei, H. Yang, Z. Gao, Y. Liu, G. Xing, P. Dang, A. A. A. Kheraif, G. Li, J. Lin, R. S. Liu, *Advanced Science* **2020**, 7, 1903060.

[17] S. He, F. Xu, T. Han, Z. Lu, W. Wang, J. Peng, F. Du, F. Yang, X. Ye, *Chemical Engineering Journal* **2020**, 392, 123657.

[18] S. Fang, T. Lang, T. Han, J. Wang, J. Yang, S. Cao, L. Peng, B. Liu, A. N. Yakovlev, V. I. Korepanov, *Chemical Engineering Journal* **2020**, 389, 124297.

[19] T. Tian, Z. Wang, C. Mao, M. Chen, Y. Chu, Y. Li, *Journal of Alloys and Compounds* **2024**, 973, 172887.